JOURNAL OF SOLID STATE CHEMISTRY 66, 116–124 (1987)

Electron Microscope Study on the New Phases of $BaMnO_{3-x}$ Substituted for Mn Sites by Some Cations

H. SHIBAHARA

Department of Chemistry, Kyoto University of Education, Fushimi-ku, Kyoto 612, Japan

Received January 10, 1986; in revised form May 5, 1986

Structures of new phases represented by the formula $BaMn_{1-x}M_xO_3$ (M = metal ion) were studied by high-resolution electron microscopy. $BaMn_{1-x}M_xO_3$ was formed by substituting M cations (M = Ta and Zn ions) for Mn ions. Electron microscope images showed that cation substitution for Mn ions in the $BaMnO_{3-x}$ system induced a phase transformation for the 2H phase into other phases with a longer periodicity than that of 2H. In the case of Ta ion substitution, the structure images showed that the structure of the 2-layer phase was transformed into a modified structure corresponding to a 15-layer phase accompanied by a shear normal to the c axis in hexagonal lattice. These results support the mechanism which was previously suggested by the present author and his colleague in the case of the phase transformation of the $BaMnO_{3-x}$ system caused by the electron beam irradiation in electron microscopy.

Introduction

The $BaMnO_{3-x}$ system is known to have a layer structure closely related to that of perovskite with oxygen deficiency. This material is based on the stacking of close-packed layers of BaO_3 with Mn metals occupying interlayer octahedral sites. The 2H (H = hexagonal) phase is a stoichiometric state and is depicted as the ABAB . . . stacking sequence characterized by infinite chains of face-sharing octahedra (Zhdanov symbol: $(\bar{1}1)$) (*1–3*).

The perovskites with the general formula XYO_3 have been extensively studied because of their interesting ferroelectric properties. The structural modifications in the oxides of XYO_3 were studied by several authors by means of X-ray diffraction. For example, the systems of $BaRu_{1-x}M_xO_3$ (M = metal ion: Zr, Mn, Ni, Mg) (*4*) and $Ba_{1-x}Sr_xRuO_3$ (*5*) were examined to find some correlation between the nature of the substituent elements and a crystal structure. The detailed study on the phases in such materials by X-ray diffraction is rather difficult, because the Y cation tends to exist as a mixture of various oxidation states. Since, however, high-resolution electron microscopy has the advantage of examining local phase relations between the layered structures in atomic scale, it seems to be useful for investigating the detailed structure of XYO_3 compounds. Thus, using electron microscope observations, the present author and his colleague suggested previously the mechanism for the phase transformation of 2H structure into non-stoichiometric states by electron beam irradiation (*3*). This proposed mechanism

0022-4596/87 $3.00

explained that the reduction by beam irradiation generates Mn^{3+} ions in octahedra with a lower coordination number and induces their displacement to avoid the electrostatic repulsion between shorter face-sharing octahedra. In order to examine the mechanism stated above, the present author studied the relation among a few phases formed by partial substitutions for Mn ions in $BaMnO_{3-x}$ by Ta or Zn ions, which have almost the same effective radii as Mn ions, using the electron diffraction patterns and the structure images formed by a high-resolution electron microscope. The results are described in this paper.

Results with the phases formed by the substitution for the Ba site in $BaMnO_{3-x}$ will be reported elsewhere.

Experimental

The 2H phase of barium manganite ($BaMnO_3$), which was used as the starting material, was prepared by the following procedure: hyperpure $BaCO_3$ and MnO_2 were mixed in an equimolar ratio under absolute ethanol for 24 hr by a magnetic stirrer. The mixtures were heated in air at 1150°C for 6 hr or at 1250°C for 10 hr in an electrical furnace and then cooled very slowly to room temperature to achieve the fully oxidized state. Subsequently, the products were mixed with weighed amounts of hyperpure tantalium oxide or zinc oxide as a tertiary component. The mixing time for preparing the mixture was 24 hr, and the mixture containing tantalium oxide or zinc oxide was heated at 1150°C for 6 hr in air and then rapidly cooled to room temperature. The sintered products were identified by using the X-ray powder diffraction method. X-Ray powder patterns of the samples were recorded by using Ni-filtered Cu$K\alpha$ radiation. For electron microscope observation, the samples were finely ground and dispersed in absolute ethanol and then mounted onto holey carbon microgrids. High-resolution electron microscope images were taken with a JEM-200CX or a JEM-2000EX electron microscope. In order to detect the difference in structure due to the stacking sequence of BaO_3 and the substitutions by some cations, a very thin fragment was selected and its orientation was adjusted so as to make the incident beam direction vertical to the c^* axis in reciprocal space by using a goniometer stage. Fast Fourier transform of a high-resolution electron microscope image was carried out to obtain the small selected area diffraction pattern.

Results and Discussion

1. X-Ray Powder Diffraction Study

The sample used as the starting material gave an X-ray powder diffraction pattern of 2H structure with a = 0 57 nm, and c = 0.48 nm, as shown in Fig. 1a, which agreed well with that of Hardy (*6*). The indices are

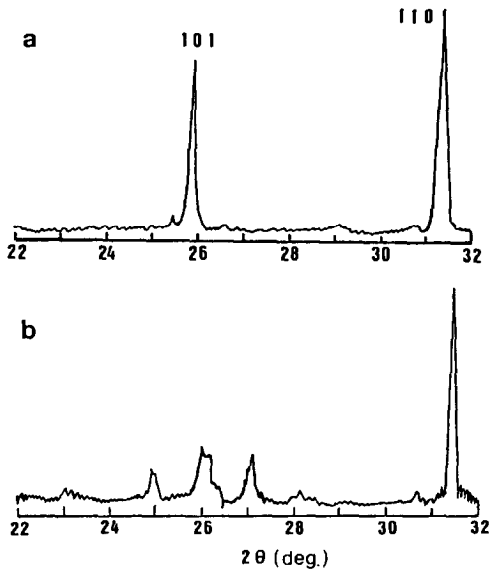

FIG. 1. X-Ray powder diffraction patterns of (a) a 2-layer phase used as starting material, the indices for which are based on a 2-layer hexagonal lattice, and (b) prolonged heating for 10 hr at 1250°C.

based on the hexagonal system of 2-layer $BaMnO_3$. With prolonged heating for 10 hr at 1250°C, a phase transformation of the 2H crystal took place which gave an X-ray powder diffraction pattern as shown in Fig. 1b.

The samples in which some metal ions were substituted were studied. Shannon and Prewitt (*8*) reported that the effective ion radii of Mn^{4+}, Mn^{3+}, Ta^{5+}, and Zn^{2+} in octahedral sites are 0.068, 0.072, 0.068, and 0.074 nm, respectively. Ta^{5+} and Zn^{2+} ions have almost the same effective radii as Mn ions in octahedra, and so they can substitute for Mn ions in a charge-compensating manner. The substitutions of Y cation with different sizes could change the effective size of the unit cell without any great structural change of the matrix while maintaining X cation constant in XYO_3. The present experimental conditions seem to be depicted by the following chemical reactions.

Ta^{5+} doping

$$Ba^{2+}Mn^{4+}O_3^{2-} + xTa^{5+} \rightarrow Ba^{2+}(Mn^{4+}_{1-2x}Mn^{3+}_{x}Ta^{5+}_{x})O_3^{2+} \quad (1)$$

Zn^{2+} doping

$$Ba^{2+}Mn^{4+}O_3^{2-} + xZn^{2+} \rightarrow Ba^{2+}(Mn^{4+}_{1-x}Zn^{2+}_{x})O^{2-}_{3-x} + \tfrac{1}{2}O_2 \quad (2)$$

The chemical reaction (1) indicates that some Mn^{4+} ions, after being substituted for partly by Ta ions, reach the trivalent state (Mn^{3+}) having a lower coordination number without any yielding of oxygen vacancies. Also the process (2) indicates that some Zn ions substitute for Mn ions by releasing oxygen gases while maintaining electric charge neutrality. In both cases it should be noted that Zn^{2+} and Ta^{5+} ions have almost the same effective ion radius as that of the Mn ion. Consequently, in octahedral sites, Zn^{2+} and Mn^{3+} ions induced by Ta ion substitutions having the effective ion radii—ions a little larger than those of Mn^{4+} (Zn^{4+}/Mn^{4+} = 1.09, Mn^{3+}/Mn^{4+} = 1.06)—

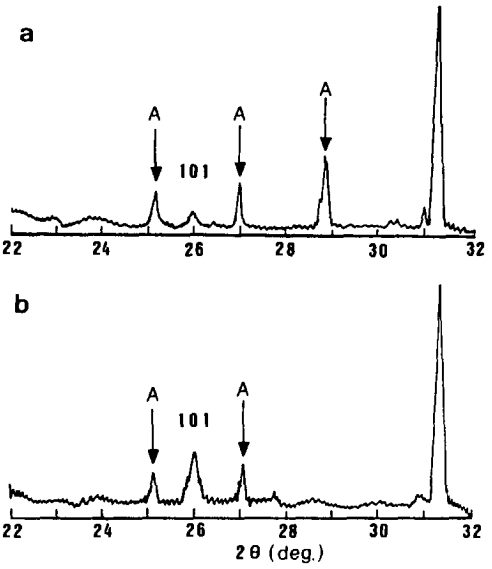

FIG. 2. X-Ray powder diffraction patterns of samples mixed with (a) Ta_2O_5 of about 0.03, (b) ZnO of about 0.06 in mole ratio to $BaMnO_3$.

are able to play an important role in creating a shear to avoid the electrostatic repulsion among neighboring face-sharing octahedra. This situation is analogous to that of phase modification introduced by electron beam irradiation (*3*). Therefore, the present experimental treatment could simulate the phase transformation of the 2H structure into another phase based on the mechanism mentioned above (*3*).

Figures 2a and b show the X-ray powder diffraction patterns of the samples mixed with Ta_2O_5 of about 0.03 and with ZnO of about 0.06 in mole ratio to $BaMnO_3$, respectively. The diffraction patterns of Figs. 2a and b show characteristic features when compared with that of Fig. 1a. The 101 line of the 2H structure in Fig. 1a has a tendency to decrease in intensity and broaden in the peak width as a result of substitution of some cations, as shown in Figs. 2a and b. The measured samples had been mixed sufficiently and well crystallized, so this tendency is due not to the insufficient mixing or sintering of the tertiary components but

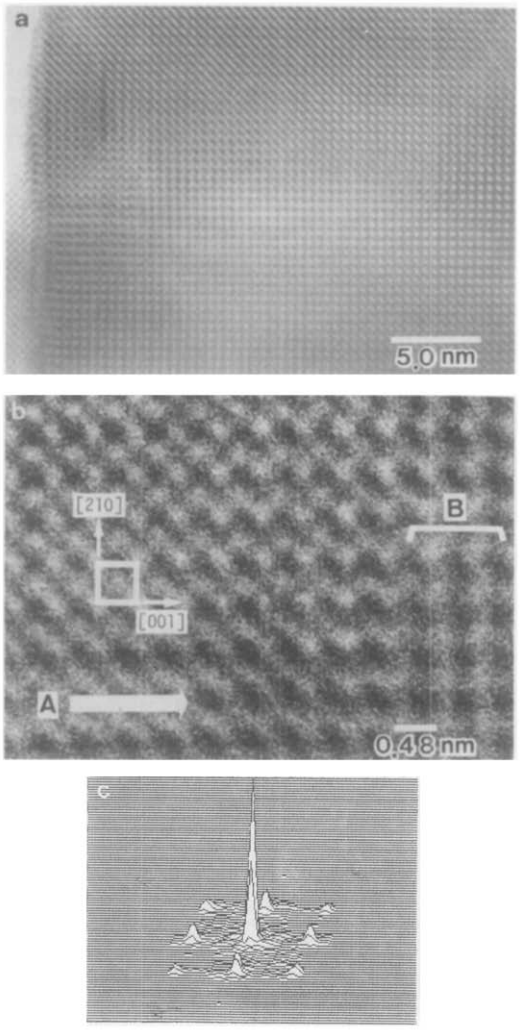

FIG. 3. Low-magnification image (a) and enlargement (b) with Fourier-transformed pattern (c) of a high-resolution electron microscope image of the 2H structure in $BaMnO_3$ taken with an incident beam parallel to the [010] direction in the hexagonal lattice. A unit cell of the 2H structure is inserted into the figure (b). The thickness of the sample increases gradually along arrow A in (b).

to the ordering of BaO_3 layers normal to the c axis in the hexagonal lattice. Some characteristic lines corresponding to other phases were also noticed in Figs. 2a and b as indicated by arrows A. Identical lines were also observed in the peaks of Fig. 1b, which agrees with the results by Negas and Roth (*1*) for samples heated between 1150 and 1300°C in air. They concluded that with increasing temperature, the 2-layer hexagonal phase transforms to a new modification which has a long periodicity along the c axis involving a progressive increase of cubic-type layer stacking. Therefore, the present samples seem to consist of a stacking of close-packed BaO_3 layers with the substituted metals occupying interlayer octahedral sites and to have a long periodicity along the c axis.

From only the X-ray powder diffraction patterns of Figs. 2a and b, the periodicity along the c axis in the hexagonal lattice cannot be examined in detail because of the mixtures with only a few phases.

2. *Electron Microscope Study*

Figures 3a and b show the low magnification and enlargement, respectively, of a high-resolution electron microscope image of the starting sample, which is identical with that of Fig. 1a. It was taken with an incident electron beam parallel to the [010] direction in the hexagonal lattice, which could be checked by Fourier-transformed pattern of Fig. 3c. The sample was not subjected to change in structure by electron beam irradiation during observation. The thickness of the sample increases gradually along arrow A as shown in Fig. 3b and the framework of the unit cell projected onto the $(1\bar{2}0)$ plane is shown in the inset. Figures 4a–i show the simulated images based on the model of the 2H structure of $BaMnO_3$ by the multislice method (*9*, *10*) under the following imaging conditions: the thickness of the sample, 5.6 nm, 13.4 nm, and 22.0 nm; Δf = 58 nm, 95 nm, and 110 nm underfocus; C_s = 1.4 mm, C_c = 1.8 mm, the beam divergence angle 1×10^{-3} rad; and the accelerating voltage 200 kV. The framework of the unit cell in the 2H structure and the model projected onto the $(1\bar{2}0)$ plane are shown in the inset. The scheme of their

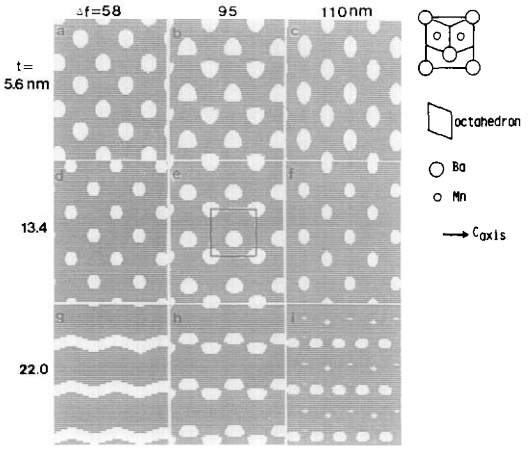

FIG. 4. Simulated images and a structure model of the 2H structure in $BaMnO_3$. They are also shown after changing both the thickness of the sample and the defocusing value in the imaging condition. The defocusing values are represented with underfocus.

simulated images led to the conclusion that, for example, in the image of Fig. 4d for Δf = 58 nm underfocus and 13.4 nm thickness the strongly bright dots represent the absence of heavy atoms such as Ba, but with increasing defocus value, they gradually correspond to the position of Ba atoms as shown in Figs. 4e and f. A series of the simulated image in Figs. 4b, e, and h, having 5.6, 13.4, and 22.0 nm thickness and taken 95 nm underfocus, is in reasonably good agreement with the observed image shown in Fig. 3b. But a little difference of image contrast in the comparatively thicker region is found. This could be interpreted by considering the contribution of forbidden reflections to image contrast due to the tilting effect of the incident beam to the specimen (*11*).

Figures 5 and 6 are the electron microscope images and the diffraction patterns of the same samples mixed with Ta_2O_5 and ZnO as those of Figs. 2a and b, respectively, which were taken with the incident electron beam parallel to the [010] direction in the hexagonal lattice. In Fig. 6a, fringes with a spacing of about 0.34 nm corresponding to the spacing of the (101) plane in a 2H phase were observed, which also had a step-like structure as indicated by arrows, revealing that a shear in the BaO_3 layers was induced by substituting Zn atoms for the Mn site. Figure 5a shows results similar to those of Fig. 6a, which not only had fringes corresponding to 2H structure as indicated by arrow A but also had the step-like structure due to the planar faults with irregular intervals in the observed image as

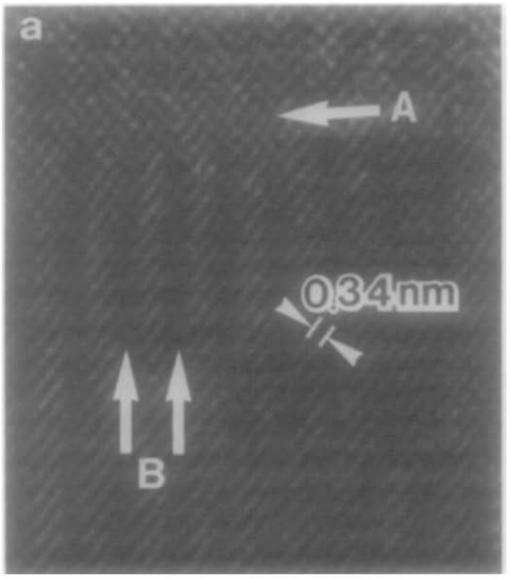

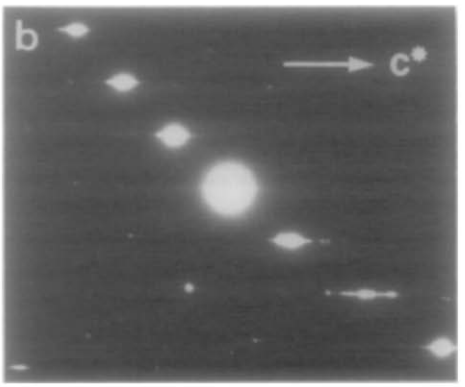

FIG. 5. Electron microscope image and diffraction pattern of the sample with Ta_2O_5.

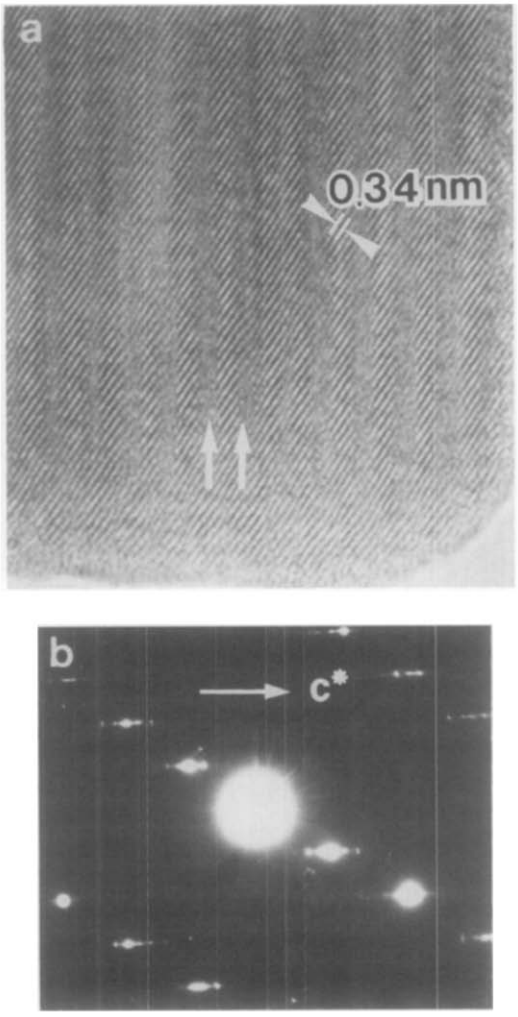

FIG. 6. Electron microscope image and diffraction pattern of the sample with ZnO.

indicated by an arrow B. The diffraction patterns of Figs. 5b and 6b also showed the streaks which could be interpreted by assuming the structure to be in the form of layers which are stacked with planar faults normal to the c axis and which have the lattice distances changed periodically.

In order to discuss the variations in image contrast due to the substitution of Ta or Zn ions for Mn sites in $BaMnO_3$, the simulations of the electron microscope image under several imaging conditions were made. Figures 7a and b show the simulated images of the samples. Here, Ta and Zn ions are assumed to be substituted for Mn sites in the 2H structure of $BaMnO_3$. The models used for simulating images are also shown. No difference is found in the simulated image contrast between Fig. 4 and Fig. 7b, since Zn atoms have almost the same power of atomic scattering as that of Mn atoms. On the other hand, the simulated image of Fig. 7a shows a more characteristic image contrast than that of Fig. 7b due to the substitution of Ta atoms which have a larger atomic number than atoms of both Mn and Ba. Thus the present author examined in detail the samples substituted with Ta atoms in $BaMnO_3$ by high-resolution electron microscopy. Figures 8a and b show an example of the low-magnification image and enlargement of the sample formed by adding Ta atoms in the form of Ta_2O_5 with about 0.05 in mole ratio to Ba

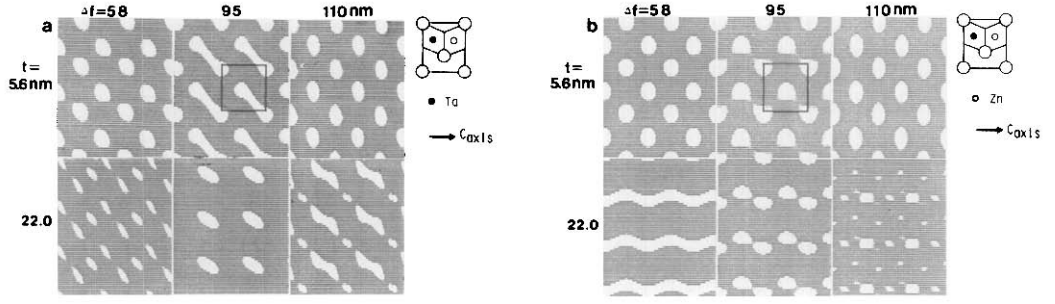

FIG. 7. Simulated images of the samples with (a) Ta_2O_5 and (b) ZnO. Structure models projected onto the $(1\bar{2}0)$ plane with substitutions by other cations for Mn sites are also shown.

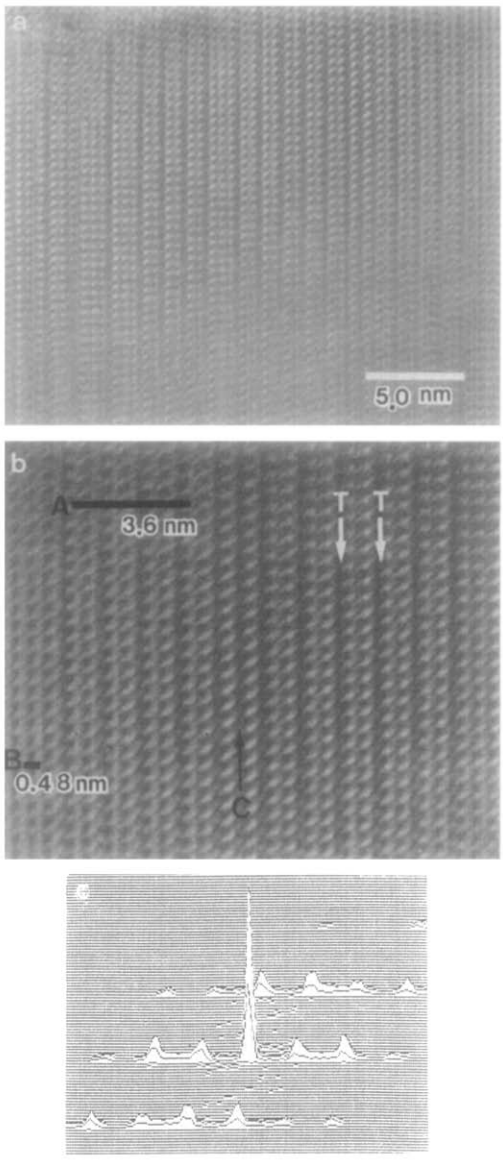

FIG. 8. Low-magnification image (a) and enlargement (b) of the sample with substitutions by Ta ions for Mn sites. A long periodicity of about 3.6 nm along the c axis in the hexagonal lattice are observed. Fourier-transformed pattern is shown in (c).

MnO_3, which were taken with the incident electron beam parallel to the [010] direction in hexagonal lattice. Figure 8c represents the diffraction pattern made by Fourier transform from the selected area. In Fig. 8b

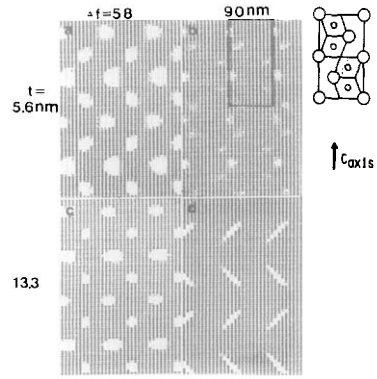

FIG. 9. Simulated image and structure model of a 4-layer structure which is the same as that of 4H-$SrMnO_3$.

the array of white spots represents periodicities of about 3.6 nm (mark A) and 0.48 nm (B) along the c axis, which corresponds to intervals of 15 and 4 times the spacing of the BaO_3 layer. And, as indicated by arrow C in Fig. 8b, irregular sequences were also found. This situation could be confirmed with streaks along the c axis in the diffraction pattern of Fig. 8c. In comparison with the simulated images under several imaging conditions, the positions of substitutions of Ta atoms for Mn sites in $BaMnO_3$ were considered as follows. Figures 9 and 10 show a

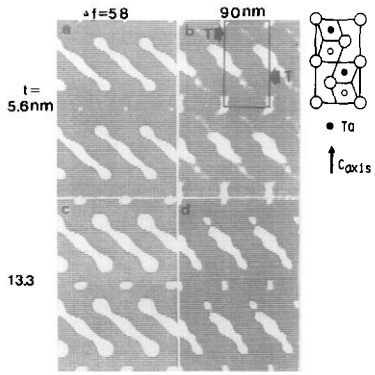

FIG. 10. Simulated image and structure model of a 4-layer structure with substitutions by Ta ions for Mn sites at positions of $Z = 0.375$ and 0.875.

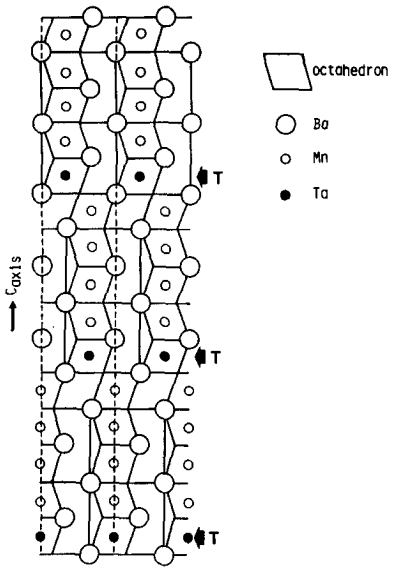

FIG. 11. A proposed structure model having a long periodicity along the c axis is projected onto the $(1\bar{2}0)$ plane of a hexagonal lattice corresponding to the observed image of Fig. 8b.

series of simulated images based on models of the 4-layer structure shown in the insets. The model used for simulation of Fig. 10 assumes that several Mn atoms located in octahedra (positions $Z = 0.375$ and 0.875) are substituted by Ta atoms without the defect due to oxygen vacancy. The 4-layer structure model of Fig. 9 contains two corner-sharing octahedra with Mn metals which is the same sequence as that of the 4H structure of $SrMnO_3$ (*12*). By comparing the feature between the simulated images and the illustrated models of Figs. 9 and 10, it is seen that the bright spots in the simulated images of Fig. 10 are elongated along the [102] direction of the 4-layer hexagonal structure and the positions substituted for by Ta atoms (arrows T) are represented by a dark region in contrast. It is also found that a clear distinction in image contrast between the simulations of Figs. 9 and 10 could be drawn. The array of white dots indicated by mark B in Fig. 8b is found to correspond to the periodicity along the c axis of the 4-layer structure shown in Fig. 10. The fringes of about 3.6 nm indicated by mark A in Fig. 8b could be interpreted as being due to the periodical substitutions of Ta atoms for Mn sites, considering the relative position of white dots in image contrast. The hexagonal structure model, having a long periodicity (15 layer), could be proposed as shown in Fig. 11. Figure 11 illustrates a model of a hexagonal structure projected onto the $(1\bar{2}0)$ plane with the lattice parameter of about 3.6 nm along the c axis, assuming that the Mn sites located in oxygen octahedra (arrows T) are substituted for partly by some Ta atoms represented by dark circles. The proposed structure model of Fig. 11 shows clearly that a shear in the BaO_3 layer with a displacement vector of $\pm\frac{1}{3}[1\bar{1}0]$ takes place and contributes to the imaging of the step-like structure in its lattice fringes. This sequence was not reported in the $BaMnO_{3-x}$ system by Negas and Roth (*1*). The proposed sequence, having a long periodicity, contains 20% cubic stacking; namely, it contains 3 of 15 layers in which corner sharing of octahedra occurs.

Acknowledgments

The author would like to express deep gratitude to Professor H. Hashimoto for valuable discussions and to thank Mrs. B. Stein for correcting the manuscript. This work has been financially supported in part by the Kazato Foundation.

References

1. T. NEGAS AND R. S. ROTH, *J. Solid State Chem.* **3,** 323 (1971).
2. Y. SYONO, S. AKIMOTO, AND K. KOHN, *J. Phys. Soc. Japan* **26,** 993 (1969).
3. H. SHIBAHARA AND H. HASHIMOTO, *in* "Proceedings, 7th Int. Conf. on Crystal Growth, Stuttgart;" *J. Cryst. Growth* **65,** 683 (1983).
4. P. C. DONOHUE, L. KATZ, AND R. WARD, *Inorg. Chem.* **5**(3), 339 (1966).

5. J. M. LONGO AND J. A. KAFALAS, *Mater. Res. Bull.* **3,** 687 (1968).
6. A. HARDY, *Acta Crystallogr. Sect. B* **15,** 179 (1962).
7. B. L. CHAMBERLAND, A. W. SLEIGHT, AND J. F. WEIHER, *J. Solid State Chem.* **1,** 506 (1970).
8. R. D. SHANNON AND C. T. PREWITT, *Acta Crystallogr. Sect. B* **25,** 925 (1969).
9. J. M. COWELY AND A. F. MOODIE, *Acta Crystallogr.* **10,** 609 (1957).
10. P. GOODMAN AND A. F. MOODIE, *Acta Crystallogr. Sect. A* **30,** 280 (1974)
11. S. NAGAKURA, Y. NAKAMURA, AND T. SUZUKI, *Japan. J. Appl. Phys.* **21,** L449 (1982).
12. T. NEGAS AND R. S. ROTH, *J. Solid State Chem.* **1,** 409 (1970).